AIRBORNE HYPERSPECTRAL SKYDOME: THE NEW DIMENSION OF HYPERSPECTRAL SENSING

Kyu-Young Choi , and Edward J. Milton

Geography & Environment, University of Southampton, Highfield, Southampton, SO17 1BJ UK – ejm@soton.ac.uk

KEY WORDS: Airborne, Hyperspectral, Atmosphere, Aerosol Optical Depth.

ABSTRACT:

A new concept of hyperspectral sensor is presented. Novel design of hyperspectral skydome allows retrieval of atmospheric constituents and properties from snapshot of direct and diffuse components of spectral solar radiation, regardless of aircraft motion under normal operational condition. Design and description of subsystems of the instrument are given followed by preliminary tolerance analysis. Details of hardware specifications and uncertainties are to be added in the retrieval algorithm. Extended application of the hyperspectral skydome is being carried out filling in the gap in the imaging spectrometry.

1. INTRODUCTION

Properties in lower part of atmosphere, i.e. troposphere and stratosphere, are an important topic in wide range of science community, such as weather, air pollution and global warming. Aerosol and trace gas studies are key to understanding the Earth's atmosphere and therefore the sustainable environment of the Earth. Generation and transport of anthropogenic (and natural) constituents are thought to be implicated in climate changes and affect human health in the form of air pollution. Since decades, complicated nature in the region has been studied 1) for net fluxes between lower and upper layers of atmosphere and 2) to understand its dynamics (Holben, et al. 1998; King et al, 1999). Various monitoring techniques have been used, such as active systems like CALIPSO, ground-based lidar, and passive systems such as sun/sky photometers. Although those approaches have its own unique capabilities and limitations, synergystic use of different approaches has been the key to improvements in radiative transfer models and retrieval algorithms (e.g. Ricchiazzi et al. 2006). Such technique on airborne platform yields unique capability, in the interest of validation of spaceborne retrievals of stratospheric and tropospheric constituents and consistency with other monitoring means for horizontal and vertical distributions of gas and aerosol properties. NASA Ames airborne tracking sunphotometers (AATS-6 and -14) with has successfully demonstrated obtaining atmospheric constituents from the Sun's direct-beam transmission through the atmosphere. Next generation airborne sunphotometer is being undertaken at NASA for gases and aerosols extending beyond its predecessor (Schmid *et al*, 2010).

Such information is also arguably essential for airborne imaging spectrometers (IS), due to 1) nonequivalent path lengths in viewing geometry, requiring additional atmospheric information at sensor altitude, 2) its normal flight altitudes around the edge of planetary boundary layer below which still plays an important role in radiative forcing sensitive to the ground reflected spectral signature, e.g. Ozone, aerosol and water vapour, and 3) high spatial and temporal atmospheric variability under the sensor altitude. Downwelling irradiation synchronised with airborne IS, e.g. ILS for Itres instrument CASI and FODIS for Specim instrument AISA, is supposed to give at-sensor spectral reflectance. This simple device needs assimilation of navigation and empirical sky radiance model to suppress aircraft motion from the irradiance at tilted surface and to retrieve basic atmospheric parameters, i.e. direct-to-diffuse ratio and skyradiance distribution at horizontal level (Choi and Milton, 2001).

The UK Natural Environment Research Council's (NERC) Strategy "Next Generation Science for Planet Earth" identified the support of the development of new and innovative technologies for environmental science, under which the Technology Proof of Concept (TPoC) programme initiated a study for the definition of an airborne hyperspectral skydome. It aims to carry out theoretical studies and to develop a prototype instrument that extends far beyond the conventional systems. To achieve the goal, the noble design with an imaging spectrometer enables to avoid complicate moving parts, like ground-based sunphotometers, which 1) quicken sky scanning, 2) increase reliability, and 3) lower the maintenance cost.

The following sections presents concept of the airborne hyperspectral skydome and its definition.

2. DESIGN OF HYPERSPECTRAL SKYDOME

Outline of skydome design is depicted in Figure 1. The fundamental of the design is to acquire both spectral irradiance and radiance over sky. While a cosine corrector covers 180º FOV for irradiance measurement (wide angle probe; WAP), total of 143 radiance probes (<5º FOV; narrow angle probe; NAP) are evenly distributed over the similar coverage of irradiance. All optical probes have unique fixed view angle on a skydome structure (DOM). Optical fibre bundle (OFB) transfers the light in the optical probes into a multi-channel spectrometer (SPEC), projecting them onto a single 2D CCD. The operation of SPEC is supported by CDHU

(Command & Data Handling Unit) and power unit (PSU). A miniature AHRS (Attitude & Heading Reference Sensor) is mounted at the skydome for position of the sensor head.

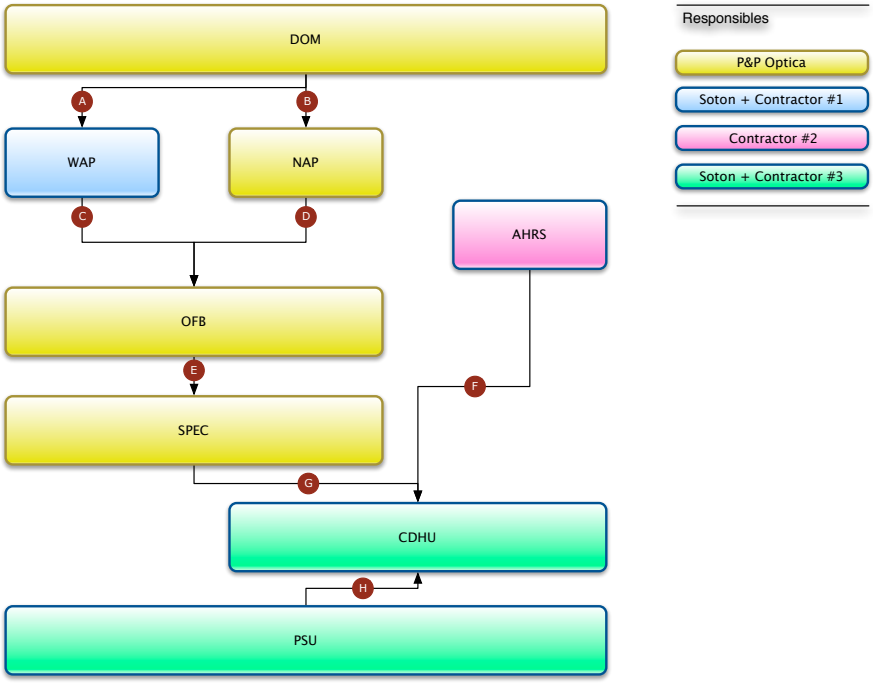

Figure 1. Schematic diagram of subsystem components in the hyperspectral skydome. Colours in the boxes represent the responsible of the subsystems, while red circles indicate identified interfaces between the subsystems.

2.1 Spectrometer (SPEC)

P&P Optica Inc offers a multichannel spectrometer, whose module takes up to 144 optical fibres (Figure 2). This portable instrument (320×120×100 mm) uses a volume phase holographic (VPH) transmission grating (470-915 nm) that enables compact system with minimal straylight. The modular system allows replacing conventional imaging fore-optics to a multi-branch fibre optic coupler in front of the entrance slit. Spatial domain of the data is effectively no longer limited by optical FOV, while maintaining the identical spectral range. For maximum number of fibres, the optical fibre is customised with 85µm diameter with 60µm core. The other end of the spectrometer has Hamamatsu camera (C10151) with 2068×512 pixels of CCD. As nominal integration time is 1 second with a mechanical shutter, lights from all fibres are simultaneously recorded.

(a)

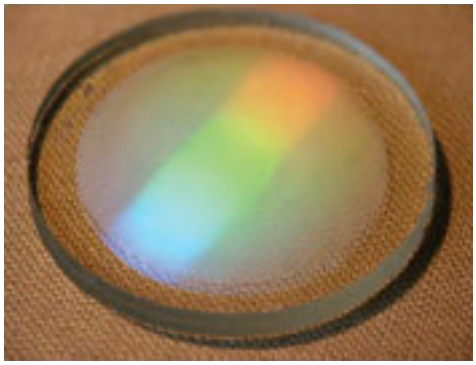

(b)

Figure 2. Multichannel spectrometer (a) and VPH transmission grating (b). Courtesy of P&P Optica Inc.

2.2 NAP (Narrow Angle Probe)

NAP is a miniature fore-optics with ±2.5° FOV, i.e. receives light from pre-determined area of interest as well as protecting optical fibres from dust or moist in the air (Figure 3a). Ray tracing analysis in Figure 4 shows that FOV of NAP is secure with wavelengths. While NAP is securely attached with a standard LC fibre connector, the unit is to hold its position in skydome. This customised triplet system minimises chromatic aberration between 400 and 1000 nm, while straylight is expected to be minimal by <1%.

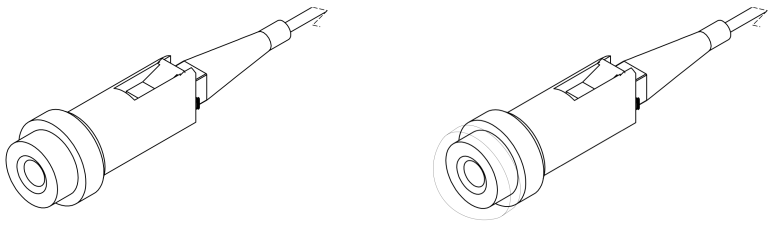

(a) (b)

Figure 3. Diagram of NAP (a) and WAP (b).

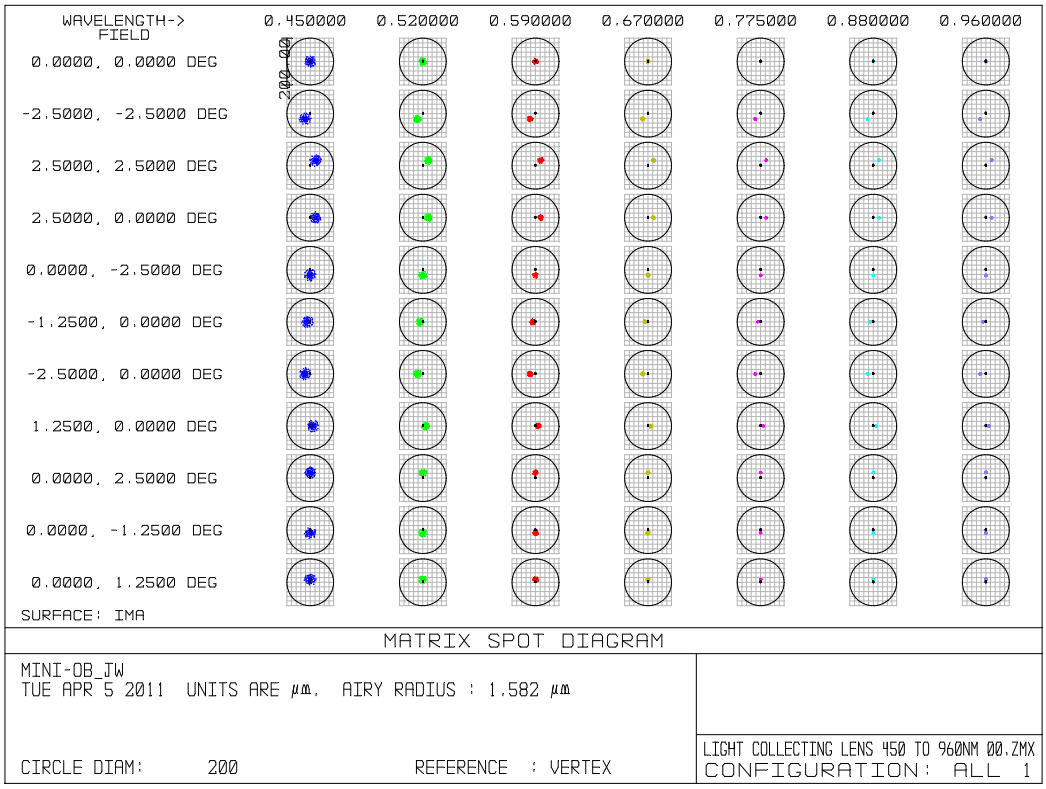

Figure 4. Spot diagrams of NAP with ranges of FOV and wavelengths.

Additional tolerance tests were made on the basis of the NAP design for the level of uncertainties, which determines in the data product. Three aspect of error sources are estimated here, i.e. PSF and FOV. Ideally, boundary of FOV is to be step function, so that region of interest within FOV is explicitly distinguished to the outside of the FOV. Due to optical properties and nature of diffused light, some level of gradual response is unavoidable. The quantitative representation of such behaviour, point spread function (PSF), is expressed by cumulative distribution function (CDF).

There are four standard deviations, σ, tested here from 0.5 to 2.0 with 0.5 intervals. Comparison of radiances at NAPs with the sharp and ideal PSF (σ=0.1) and the variable sigma, yields the % differences as an error induced by the new PSF. Figure 5a shows that the smoother the PSF boundary the more errors in overall NAPs. Errors induced by PSF are however not significant, relative to the others. At σ=2.0, NAP is sensitive up to ±3.6 degree FOV although half-maximum value remains at ±2.5 degree from optical axis. Even in this condition, maximum error is still less than a twentieth of a percent.

Given FOV of NAP is focused on a core of optical fiber, diameter of 60μm. Minute displacement and lens tolerance introduce FOV changes. Unverified non-uniform FOV in NAPs can be a problematic not only for radiance at each NAP, but also to derive hemispheric irradiance. A range of FOV is set, ±2.0~3.0 with 0.1 degree interval. Figure 5b shows % difference of measurement with variable FOV over the ones from reference FOV. Box plots from left to right tend to increase median values as FOV increases. While minimum and maximum ranges increase dramatically, errors within <±0.5 degree are generally small. Nonetheless, care should be taken because errors from FOV tolerance becomes much greater at high spatial variable region of the sky, such as near the Sun. Min/Max values in the box plots are related to the Solar angle.

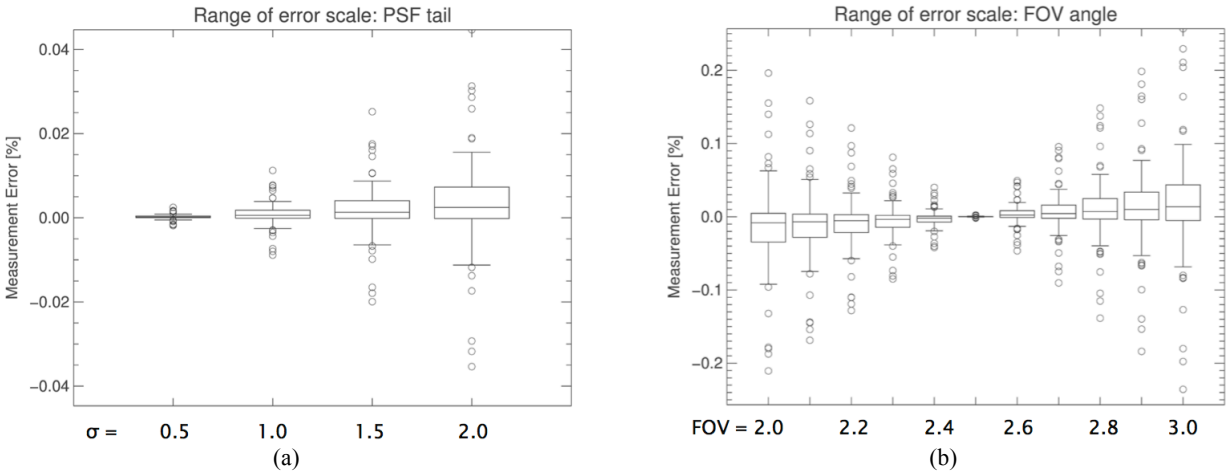

Figure 5. Box plots of tolerance analysis for PSF (a) and FOV of NAP (b).

2.3 WAP (Wide Angle Probe)

WAP is a cosine corrector with <180° FOV. It uses the same optical component as NAP since it has good chromatic aberration. Wide FOV is achieved by an additional PTFE at front aperture (Figure 3b). Optimal shape of the diffuser is to be found by stochastic photon transfer analysis for best performance.

2.4 Skydome (DOM)

The dome is an aluminium structure with 208×180 mm that maintains view angles of all optical probes. The spherical curvature of the dome is extended 20° below horizon. Hence, the radiance probes in skydome maintains downwelling irradiance at horizontal level even if the dome is tilted up to 20° (Figure 6).

Conventional angular measurements with a single probe with mechanical scanning system have equal angular intervals on both zenith and azimuth directions due to controlling mechanical system, resulting angular distance between measurements becomes dense toward the zenith of the sky (Schopfer *et al*, 2008). Such sampling strategy likely causes uncertainty in spherical interpolation, especially when FOV of the probe is greater than the sampling intervals.

To avoid the problem, NAP is to be evenly distributed over the dome. The uniform discrete sampling over sphere has been a challenge in mathematics and engineering, for example, biological protein docking, planetary observation, and quantum computations. Amongst several proposed solutions, Special Orthogonal group method (SO3) is used for NAPs (Yershova *et al*, 2009). Angular distance between NAPs is 13.73±0.66°.

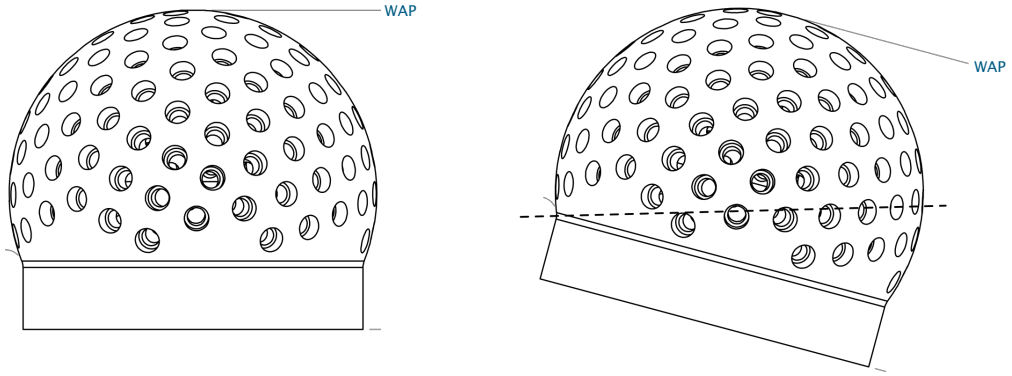

Figure 6. Diagram of skydome at horizon (left) and at 20º tilt (right). Holes in the diagram are for NAP and position of WAP is indicated in the diagram.

Tolerance of DOM design is directly related to data product, as well as optical specification of NAP. Misalignment of NAPs on DOM other than known geometry results incorrect view of sky. Its quantitative error is entirely dependent on spatial distribution of sky radiance. Optical axis of NAP passes on the centre of the dome structure, able to reconstruct the sky irradiance at a point simultaneously. NAP with the angle and direction offset is effectively looking at the relative direction equivalent to the same offset angle. The shift of the virtual focal point back to the origin shows that the NAP is effectively pointing different direction (Figure 7a). With radiance distribution under standard clear sky condition, off-axis error greater than 1° is responsible for total error >1%. This is much greater than other error factors for NAP.

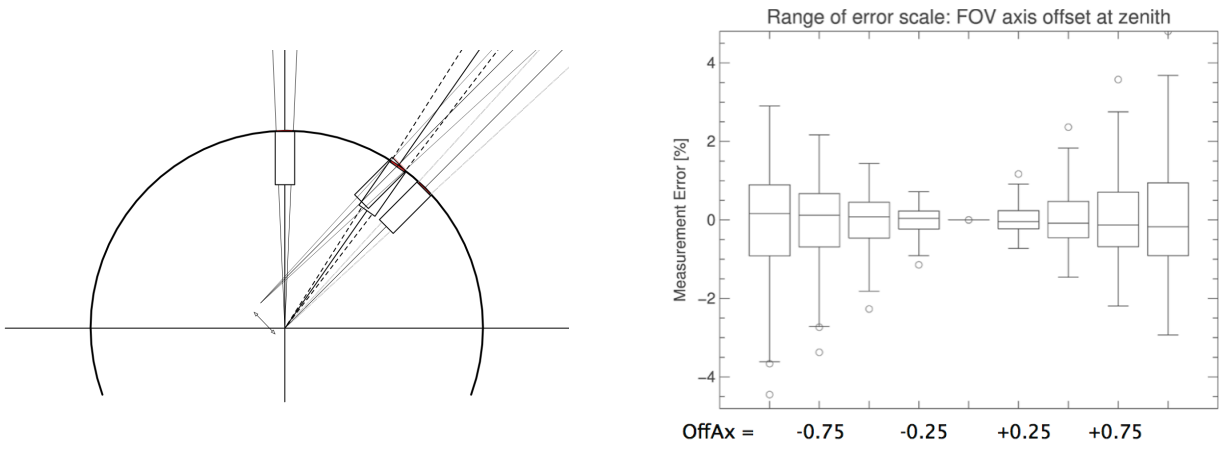

(a) (b)

Figure 7. Schematic diagram of off-axis NAP (a) and box plot of off-axis analysis.

3. BASICS OF RETRIEVAL ALGORITHM

Basic concept of conventional sunphotometer is direct-mean spectral solar radiance, transmittance of which from that of top-of-the-atmosphere (TOA) is directly related to the atmospheric effect in the atmosphere. All secondary reflection and absorption in the atmospheric constituents appears as diffused component of solar radiation,

$$E_{diff} = \int_{\Omega} L(\theta, \phi) d\omega \tag{1}$$

In other words, total solar irradiance is sum of direct and diffuse components,

$$E_{total} = E_{diff} + E_{dir} \tag{2}$$

Since the hyperspectral skydome spectrometer takes direct measurements of total irradiance (E_{total}) and diffuse radiation (E_{diff}) by integral of NAP readings (Equation 1), direct component of solar radiation (E_{dir}) can be indirectly retrieved by Equation 2. Pagnutti et al (2006) successfully demonstrated that such indirect derivation of direct-beam solar radiation has potential for alternative sunphotometer.

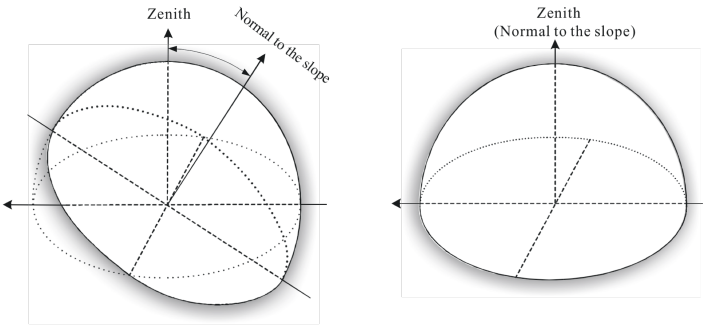

(a) (b)

Figure 8. Schematic diagram of sky hemisphere on slope (a) and horizontal plane (b).

3.1 Solar radiation at Tilt Position

Novel design of skydome extends the concept of indirect method when the skydome is on a tilted platform. As total irradiance from WAP is at the zenith of the skydome, comparison of integral of NAPs ($E_{diff}^{tilt(nap)}$) within the WAP response angle to WAP ($E_{diff}^{tilt(nap)}$) yields direct component of solar radiation (E_{dir}). Derivation of direct radiation requires radiative transfer model for aureole (e.g. Thuillier et al, 2005).

3.2 Solar radiation at Horizontal Position

While direct component of solar radiation (E_{dir}) derived above remains constant, diffuse radiation at horizontal plane is obtained by integral of NAPs above horizon ($E_{diff}^{hor(nap)}$, Figure 6 & 8b). The comparison of $E_{diff}^{hor(nap)}$ with E_{dir} represents direct-to-diffuse ratio, and the total solar radiation on a tilted plane is sum of these components,

$$E_{total}^{hor} = E_{diff}^{hor(nap)} + E_{dir} \quad (2)$$

3.3 Atmospheric Parameters

In conventional sunphotometers, sky radiance distribution from scanning gives more details of atmospheric parameters, such as aerosol size distributions, sphericity, and absorption. The derived solar radiation components will be input to a standard model.

4. CONCLUSION

Novel design of airborne hyperspectral skydome is introduced as a replacement of conventional sunphotometers. While with no moving part, the new skydome is capable of snapshot of sky radiation and aircraft motion can be compensated. Successful demonstration of the prototype instrument will be followed by operation of the skydome on the aircraft in early 2012.

Applications of hyperspectral skydome are not restricted for airborne operation. It is a spectrometer with extended geometric flexibility. Many operational issues from imaging spectrometry are often from unknowns in 3D interaction of solar radiation field that is beyond the imager's limited FOV, such as BRDF. For example, the down-looking hyperspectral skydome on aircraft, i.e. moving platform, provides broader geometric ranges of BRDF samples. Study of the potential applications is taking place in parallel with developing prototype instrument.

REFERENCES

Choi K.Y. and Milton E.J., 2001, A model-based approach to correcting spectral irradiance data using an upward-looking airborne sensor (CASI ILS). In, RSPS2001: Geomatics, Earth Observation and the Information Society. 1st Annual Meeting of the Remote Sensing and Photogrammetry Society. Nottingham, UK, Remote Sensing and Photogrammetry Society, 64-75.

B.N. Holben, T.F. Eck, I. Slutsker, D. Tanré, J.P. Buis, A. Setzer, E. Vermote, J.A. Reagan, Y.J. Kaufman, T. Nakajima, F. Lavenu, I. Jankowiak, and A. Smirnov., 1998, AERONET-A Federated Instrument Network and Data Archive for Aerosol Characterization - An Overview, Remote Sensing of Environment, 66(1), 1-16.

King, M., Kaufman, Y., Tanré, D., Nakajima, T., 1999, Remote Sensing of Tropospheric Aerosols from Space: Past, Present, and Future, Bulletin of the American Meteorological Society, 80(11), 2229-2260.

Mary Pagnutti, Robert E. Ryan, Kara Holekamp, Gary Harrington, and Troy Frisbie, 2006, Novel Hyperspectral Sun Photometer for Satellite Remote Sensing Data Radiometric Calibration and Atmospheric Aerosol Studies, NASA Stennis Space Center, Report no. SSTI-2220-0063, 48p.

Ricchiazzi, Paul, Gautier, Catherine, Ogren, John A., Schmid, Beat, 2006, A comparison of aerosol optical properties obtained from in situ measurements and retrieved from Sun and sky radiance observations during the May 2003 ARM Aerosol Intensive Observation Period, J. Geophys. Re., Vol. 111, 13p.

Schmid, B., Flynn, C., Dunagan, S., Johnson, R., Russell, P. B., Zavaleta, J., Redemann, J., Kluzek, C., Holben, B., 2010, 4STAR Spectrometer for Sky-scanning Sun-tracking Atmospheric Research: Development and Results from First Test-flights, American Geophysical Union, Fall Meeting 2010, abstract #A11I-03.

Jürg Schopfer, Stefan Dangel, Mathias Kneubühler and Klaus I. Itten, 2008, The Improved Dual-view Field Goniometer System FIGOS, Sensors, 8, 5120-5140.

G Thuillier, Sabatino Sofia, and Margit Haberreiter, 2005, Past, present and future measurements of the solar diameter, Advances in Space Research, 35, 329-340.

Anna Yershova, Steven M. LaValle, and Julie C. Mitchell, 2009, Generating Uniform Incremental Grids on SO(3) Using the Hopf Fibration, International Journal of Robotics Research, 29, 9, 18p.

ACKNOWLEDGEMENTS

The research project is sponsored by UK NERC (Natural Environment Research Council) (Ref. NE/H002235/1). Authors thank the Romuald Pawluczyk and Thomas Hummel in P&P Optica Inc for technical support and information of the optical components of the

hyperspectral skydome instrument. Andreas Hueni and Mathias Kneubühler in RSL, University of Zurich kindly provide FIGOS goniometer data.